Desalination and Water Treatment
www.deswater.com

doi: 10.1080/19443994.2016.1184592

57 (2016) 28313–28322
December

Taylor & Francis
Taylor & Francis Group

Adsorption kinetic and mechanism studies of thorium on nitric acid oxidized activated carbon

Nafisa A. Salem[a,*], Sobhy. M. Ebrahim Yakoot[b,1]

[a]*Ministry of Higher Education and Scientific Research, Cairo, Egypt, Tel. +20 1007116122; email: nsalem2030@gmail.com*
[b]*Biochemistry Department, College of Science, King Saud University, P.O. Box 2455, Riyadh 11451, Kingdom of Saudi Arabia, email: sebrahim2016@gmail.com*

Received 28 November 2015; Accepted 21 April 2016

ABSTRACT

Rice straw activated carbon oxidized with HNO_3 was studied for thorium removal. It was found that carbon has mesoporosity (82%) greater than microporosity (18%) and high ash content (54.1%). Acidic oxides including carboxyl, lactonic, and phenol ones are formed on the carbon surface during preparation and oxidation. The thorium adsorption process proves that the rate of reaction was fast, requiring short contact time. Optimum values were set as pH of 4.0 and 20 mg/l for thorium at removal time of 100 min. Different models were used to determine the kinetic data among which a pseudo-second-order equation was the best fit ($R^2 = 0.999$). The mechanism of the adsorption kinetics was investigated by employing intra-particle diffusion, surface mass transfer, and Boyd kinetic expressions. The results show that thorium ions' transportation from solution to the surface of the adsorbent is rapid enough (6.2×10^{-6} cm/min) to use these residues for the removal of thorium from contaminated wastewater. Particle diffusion is the best operating mechanism to control the sorption kinetics of thorium ions. Used carbon had comparable adsorption capacity for thorium as compared to other adsorbents. The quantitative elution study of thorium can be realized with sulfuric acid. Consequently, this carbon can be considered a potentially cheap and operative scavenger for adsorption of thorium from solution.

Keywords: Thorium; Adsorption; Kinetics; Oxidized activated carbon

1. Introduction

Thorium is a naturally occurring tetravalent actinide element. It occurs in geologic materials as a trace constituent in the form of oxide, silicate, and phosphate minerals. The only known natural thorium isotope is ^{234}Th, but ^{230}Th and ^{238}Th can be found as radiogenic decay products [1]. Thorium compounds are produced from processing of rare earth minerals like monazite. A small portion of thorium produced is consumed, but most is discarded as waste. Thorium has been widely used in many applications [2] such as lighting, welding electrodes, ceramics, refractories, and metallurgical applications. Thorium oxide (ThO_2), or thoria, is used in the manufacturing of ceramics and in high-temperature/strength alloys, as it has high temperature characteristics. Most of these applications create solid and liquid wastes that include thorium isotopes. Furthermore, nuclear fuel

*Corresponding author.

[1]Present address: Atomic energy Authority, Hot Laboratories Center, 13759 Cairo, Egypt.

production also creates liquid and solid thorium wastes.

A number of different studies have been done on radioisotope removal from aqueous solutions using adsorption on various adsorbents including zeolites, silicate, titanate, antimonite, and activated carbon [3–9]. Among adsorbents, activated carbon is one of the most extensively used commercially in purification and separation [9]. Activated carbons contain surface oxygen functional groups that are able to sorb various metal ions from aqueous solutions. Moreover, their great chemical, radiation, and heat stability, along with their high mechanical strength due to a rigid porous structure, give them a great advantage over polymeric materials [10].

This study presents data and a discussion regarding thorium adsorption on nitric acid oxidized rice straw-based activated carbon.

2. Experimental activated carbon preparation

Activated carbon was processed using a method described previously [11]. Concisely, a known weight of dried raw material (rice straw) was put into a fluidized bed furnace, with a heating rate of 5°C/min in a nitrogen deficient environment (300 ml/min). Heating goes up to 550°C and is held for 1.0 h. Steam (5 ml/min) was going to the reactor at a temperature of 350°C. The prepared carbon undergoes chemical treatment using HNO_3 to give oxidized carbon labeled as RSN [12,13].

The porosity and surface area of RSN carbon were measured using nitrogen adsorption isotherms (Quantachrome Instruments, USA). The pH_{pzc} of RSN carbon was measured using simple mass titration method [14]. Acidic and basic characteristics of RSN carbon were estimated using Boehm titration method [15].

2.1. Sorption investigations

RSN carbon (5 mg) was shaken with 5 ml of thorium solution in a shaker at 25 ± 1°C for different time intervals. Then the RSN carbon was removed by filtration and the thorium concentration was measured. Blank samples without RSN carbon were done to ensure that there was no precipitation during the adsorption experiment.

To investigate the influence of pH on sorption, these experiment was done at various initial pH (2–9) of thorium solution. Initial solution pH was regulated by gradual addition of drops of 0.1 N NaOH or HCl solutions. All adsorption experiments were done at constant ionic strength of 0.1 M maintained with potassium chloride.

The effect of radionuclide ion concentration was studied by agitation of 10 ml of different concentrations (5–100 mg/l) of thorium solution with 5 mg of RSN carbon for 2 h equilibrium time. The amount of thorium adsorbed on RSN carbon was calculated by [16]:

$$q_e = \frac{V(C_o - C_e)}{m} \quad (1)$$

Sorption efficiency of thorium on RSN carbon was calculated by:

$$R\% = \frac{C_o - C_e}{C_o} \times 100 \quad (2)$$

where C_e and C_o are equilibrium and initial concentration (mol/l), respectively, V is the volume of solution (l), and m is the mass of dry carbon sample used (g).

2.2. Desorption experiments

After saturation of RSN carbon by the thorium ions, the suspension was separated and the thorium-laden RSN carbon was washed in distilled water. The stripping was realized by contact of the suspension with 10 ml of desorping agent for one day and then separated by filtration. The desorbable amounts of metal ions expressed as amount desorbed (q_{des}) or fraction desorbed ($R_{des}\%$) were calculated as follows:

$$q_{des} = \frac{VC_{des}}{m} \quad (3)$$

$$R_{des}\% = \frac{q_{des}}{q_{ads}} \times 100 \quad (4)$$

with C_{des} the concentration of desorbed radionuclide.

3. Results and discussion

Surface chemistry modification of carbons may be a worthwhile use for their unique applications. Porosity and surface area of carbon produced in this study was low compared to that of commercial carbons. For that reason, surface modification for these carbons has been done using nitric acid to get high thorium adsorption capacity. Physicochemical properties of RSN carbon are shown in Table 1. RSN carbon has mesopore volumes four times greater than micropore volumes, and its mesoporosity characteristics were more

Table 1
Physicochemical characteristics of RSK carbon

S_{BET} (m^2/g^a)	87.2
Micro-surface area fraction[a]	0.51
Meso-surface area fraction	0.49
Total pore volume (cc/g)	0.118
Micro- pore volume fraction[b]	0.18
Meso-pore volume fraction	0.82
Pore radius (nm)	2.7
Basicity (meq/g)	2.8
Acidity (meq/g)	8.93
Carboxyl (meq/g)	0.8
Lactonic (meq/g)	3.8
Phenolic (meq/g)	4.3
pH_{pzc}	3.0
Ash content (%)	54.1

[a]Brunauer–Emmett–Teller (BET) surface area.
[b]Density functional theory (DFT) Micro-surface area or pore volume fraction.

predominant than microporosity. Carbon mesoporosity facilitates and improves radionuclide adsorption.

The high ash content (54.1%) of RSN carbon may be due to destruction of a large quantity of carbon throughout the activation process that causes increased mineral content, especially silica. Carbon surface functional groups are significant factors that affect its metal adsorption capacity [17]. Coexistence of basic and acidic sites on the RSN carbon surface implies its amphoteric nature. Furthermore, iRSN carbon functional groups are determined using Boehm titration method [18], and the results were that it has three categories of acidic surface oxides (carboxylic, phenolic, and lactonic) given in Table 1.

3.1. Effect of agitation time on thorium adsorption

Fig. 1 displays the influence of reaction time on the removal of thorium by RSN. The curve produced is smooth, is single and continues until saturation, signifying the development of thorium monolayer coverage on the RSN carbon surface. Adsorption of thorium increases with time and reaches equilibrium at 120 min, which was in line with previous results [19,20]. Short uptake time is vital for use of any adsorbent in the removal process [21] and is one of the significant considerations for efficient wastewater treatment applications. Accordingly, 2 h as the optimum agitation period for thorium removal was used for the subsequent experiments to attain equilibrium.

The curves in Fig. 1 show a double nature that means that the process of adsorption occurs in two stages: a quick initial stage and after that a much

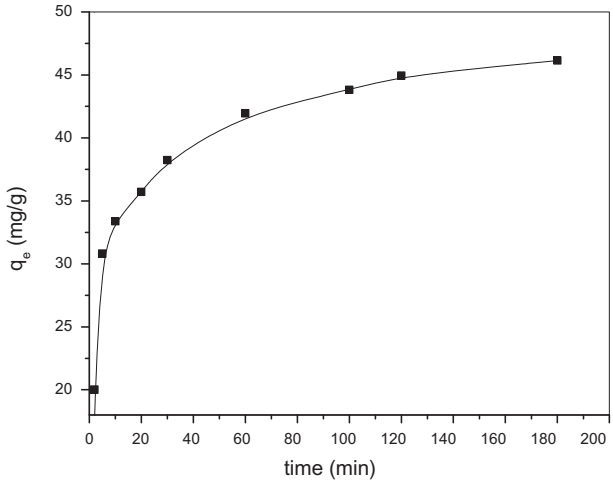

Fig. 1. Effect of time on adsorption of thorium.

slower one. Thorium adsorption on RSN carbon was very fast through the first 20 min of contact, while about 75% of the thorium was adsorbed after an additional 100 min to reach equilibrium. These two steps were also reported earlier by Tran [20]. Tang et al. explain the two-stage adsorption: during the first stage, thorium is adsorbed on the external adsorbent surface where the resistance toward its ions to reach these surfaces is small. As the adsorption proceeds, more and more radionuclide ions diffuse through macropores, mesopores, and micropores to reach the total surface area within the residue particles. However, the rate of diffusion in such pores decreases with time, and consequently the adsorptive capacity increases more slowly as time elapses until equilibrium is attained [22].

3.2. Kinetic rate parameters

According to the results obtained, the kinetic rate constant of thorium adsorption can be treated by the pseudo-first-order rate of Lagergren and pseudo-second-order rate expression as applied by Ho and McKay [23]:

$$\log(q_e - q_t) = \log(q_e) - \frac{k_1}{2.303}\, t \quad \text{First Order} \tag{5}$$

$$\frac{t}{q_t} = \frac{1}{k_2\, q_e^2} + \frac{t}{q_e} \quad \text{Second-order} \tag{6}$$

where q_t and q_e (mg/g) are the amount adsorbed at time t and at equilibrium, respectively. K_1, K_2 is the rate constant of the first- and second-order equation,

respectively. K_1 can be gotten from the straight line of plot $\log(q_e - q_t)$ vs. t from Eq. (3) and K_2 from Plot t vs. t/q_t from Eq. (4). The results of the kinetic plots are shown in Figs. 2 and 3. Table 2 lists all results that

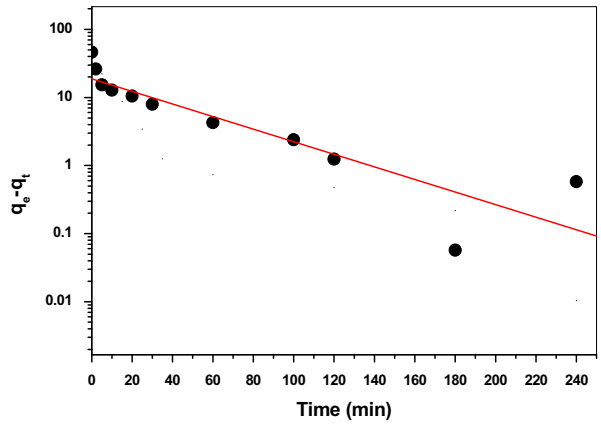

Fig. 2. Pseudo-first-order sorption kinetics of thorium.

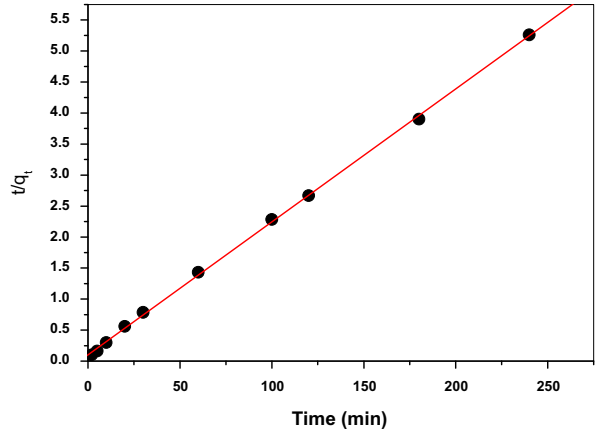

Fig. 3. Pseudo-second-order sorption kinetics of thorium.

Table 2
Assessment of the pseudo-first-, second-order rate constants, calculated and experimental q_e values for Th(IV) adsorption onto RSN carbon

Model	Parameter	
First-order model	$q_{e,exp}$ (mg/g)	46.2
	K_1 (min^{-1})	0.021
	$q_{e,cal}$ (mg/g)	19.95
	R^2	0.8
Second-order model	K_2 (g/mg min)	4.6×10^{-3}
	h (mg/g min)	10.0
	$q_{e,cal}$ (mg/g)	46.64
	R^2	0.999

were calculated for kinetic parameters K_1, K_2, $q_{e,calc}$ and the initial adsorption rate ($h = k_2 q_e^2$) with the corresponding correlation coefficients.

The first-order kinetic equation gives low values of correlation coefficient ($R^2 = 0.8$) and calculated q_e in relation to experimental q_e values. This suggested that thorium adsorption is not a first-order reaction that cannot describe the adsorption process as a whole.

Pseudo-second-order rate expression gives a good correlation coefficient ($R^2 = 0.999$), and there is good agreement between calculated q_e and the experimental one. This observation indicates thorium adsorption can be approached by pseudo-second-order, so that the pseudo-second-order adsorption mechanism is dominant and chemisorption is most likely to control the adsorption process [24].

The reactions including pseudo-second-order are significantly influenced by the radionuclide quantity on the adsorbent surface and that adsorbed at equilibrium. In other words, the reaction rate is directly proportionate to the number of active sites on the adsorbent surface [25]. RSN carbon has great adsorption capacity, q_e, that give rapid rates of adsorption and short equilibrium time. Both short equilibrium times and high adsorption capacity designate a high degree of affinity between thorium ions and RSN carbon [26].

3.3. Surface mass transfer coefficient

Data of sorption kinetics were used more to identify whether film diffusion or intra-particle diffusion is the rate-limiting step in the adsorption process.

The kinetic model described by Mohan and Singh can be expressed as follows [27]:

$$\ln\left(\frac{C_t}{C_o} - \frac{1}{1 + m K_L}\right) = \ln\frac{m K_L}{1 + K m_L} - \frac{1 + m K_L}{m K_L}\beta_L S_s t \tag{7}$$

where C_t is metal concentration at time t and zero time (mg/l), respectively. The carbon mass in unit volume of solution (g/l) is m. K_L is the constant equal of $q^o \times b$ of the Langmuir equation (l/g). β_L is the factor of mass transfer (cm/s). S_S is the carbon outer surface per particle-free solution unit volume (cm^{-1}), calculated by:

$$S_s = \frac{6m}{D_a d(1 - \varepsilon)} \tag{8}$$

where D_a is the carbon particle mean diameter (cm); d = carbon density (g/cm^3) and ε = carbon porosity.

The straight line graph in Fig. 4 results from plotting of $\ln(C_t/C_o - 1/1 + mK_L)$ vs. t proposes effectiveness of McKay equation for the current adsorption system. B_L was calculated from the slope and intercept of each plot and found to be 6.2×10^{-6} cm/min for thorium onto RSN carbon. The presence of some linearity deviations at initial adsorption stages confirms our finding that several rate-controlling steps are in the present adsorption system [28].

Further, the values of mass transfer coefficient point to that the velocity of Th(IV) transportation from solution to carbon surface is rapid enough for use of these residues for the removal of thorium from contaminated wastewater. The process may be recommended for the treatment of these radionuclide-rich wastewaters on a large scale.

3.4. Intra-particle diffusion

In Weber et al. model, the intra-particle diffusion rate as a function of $t^{0.5}$ can be expressed as follows [29]:

$$q_t = k_p t^{0.5} \tag{9}$$

The intra-particle diffusion rates (k_p) can be calculated from the q_t vs. $t^{0.5}$ plot as given in Fig. 5. Intra-particle diffusion is a rate-controlling step for linear plot that going through origin. In Fig. 5, plot has an initial curved portion, followed by an intermediate linear portion and a plateau. The initial portion is owing to external-mass transfer, the middle linear portion is because of intra-particle diffusion, and the plateau is due to equilibrium in which intra-particle diffusion starts to slow owing to extremely low solute concentrations in the solution [30].

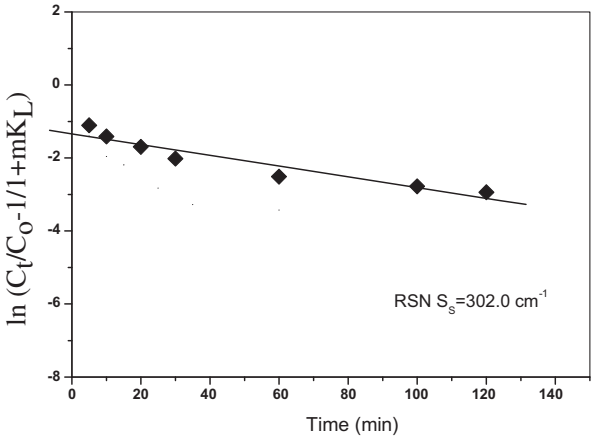

Fig. 4. Mass transfer plots for the adsorption of thorium.

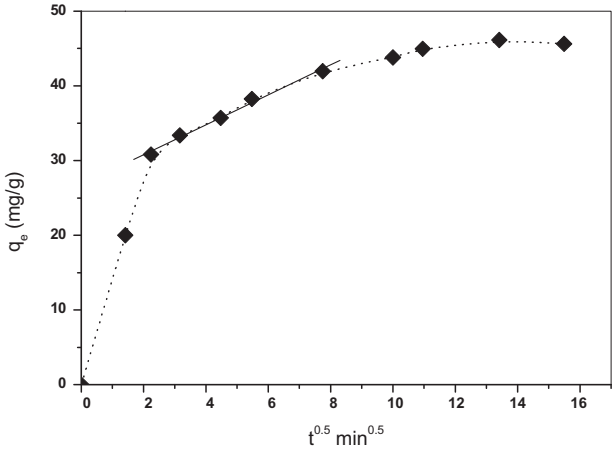

Fig. 5. Intra-particle diffusion plots for thorium adsorption.

The slope of the linear part represents intra-particular diffusion rate parameter (k_p) that equals 2.0 mg g^{-1} $min^{-0.5}$. If the intra-particle diffusion is the only rate-limiting step, it is necessary for the q_t vs. $t^{0.5}$ graph to go through the origin, which does not happen in the current work, and q_t vs. $t^{0.5}$ plots give intercepts [31]. Consequently, the intra-particle diffusion is not the single rate-controlling step. The adsorption mechanism of these radionuclide ions from aqueous solution is a rather complex process, probably a combination of external-mass transfer and intra-particle diffusion which contribute to the rate-determining step [32].

By way of the multi nature of intra-particle diffusion, the plot proves the presence of both pore and film diffusion. In order to expect the actual slow step contributed, the kinetic data were further analyzed using the Boyd kinetic expression [33]. This model can used to predict the actual slowest step in the sorption process. The Boyd kinetic model can be given by:

$$F = 1 - (6/\pi^2)\exp(-B_t) \tag{10}$$

and

$$F = \frac{q_t}{q_\infty} \tag{11}$$

where q_t and q_∞ denote the quantity of adsorbed radionuclide (mg/g) at time t (min) and infinite time, respectively, F denotes the portion of adsorbed solute at time t. B_t can be calculated using the Reichenburg equation as follows [34]:

$$B_t = -0.4977 - \ln(1 - F) \tag{12}$$

Linearity of the B_t vs. time graph can be used to differentiate adsorption controlled by particle diffusion and by film diffusion. Adsorption can be controlled by the particle diffusion mechanism if this plot (of slope B) gives a straight line going through the origin; otherwise it is controlled by film diffusion [34].

The plot of thorium adsorption in Fig. 6 is a straight line up to 120 min. However, this straight line did not pass through the origin in line with the results obtained from the Weber–Morris equation. Thus, particle diffusion was the most possible working mechanism and did not cover thorium adsorption kinetics [35]. That is to say, external mass transport primarily controls the rate-limiting process [36].

3.5. Effect of initial concentration on thorium adsorption

Fig. 7 shows thorium adsorption onto RSN carbon at various initial concentrations (5–100 ppm). It is clear that as the thorium initial concentration increased, its adsorption capacity (q_e) increased until saturation. The adsorption process appears to go on quickly when the number of available adsorption sites is greater than the adsorbable thorium ions and favorable sites involved in adsorption first. As thorium concentration increases, high-affinity sites reach saturation earlier than low-affinity and less energetic ones, causing decrease of thorium removal efficiency [37].

On a relative basis, however, the percentage of removal ($R\%$) was high at lower initial concentrations and low at higher initial concentrations (Fig. 7). In diluted solutions, the mobility of thorium ions is high, and therefore maybe the ions' interaction with the adsorbent was increased [38]. By increasing thorium concentration, hydrolyzation of its ions can increase and cannot reach adsorbent sites [39].

These results obviously show that thorium removal from the aqueous solution was dependent on its concentration. At low concentrations (below 20 mg/l for thorium), sorption was 85–95%. This suggests that rice straw carbon oxidized by HNO_3 can take most of the Th(IV) from water if its concentration is below 20 mg/l. This high thorium removal at low concentrations is significant in industrial applications.

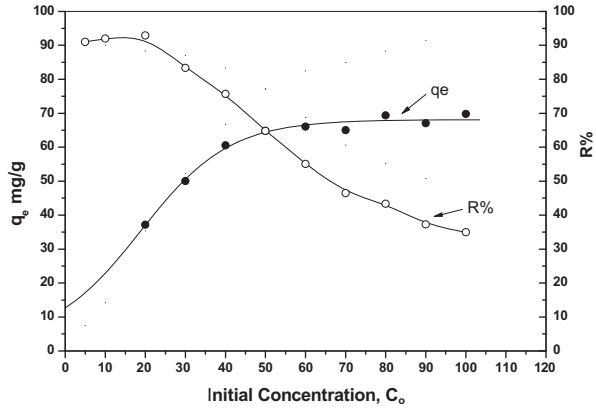

Fig. 7. Influence of initial concentration of thorium on percentage adsorption (R %) and equilibrium uptake (q_e).

3.6. Effect of solution pH on thorium adsorption

The solution pH influences on both metal speciation and its binding sites to the adsorbent surface [38]. As clearly shown in Fig. 8, the adsorption of thorium ions was markedly affected by pH of the solution. Even at low pH, RSN carbon eliminates 50% of thorium. With increasing pH, the percentage of adsorption removal increases up to a certain point (pH 4), then falls with further increase in pH.

RSN adsorbents showed amazing thorium sorption even at low pH values, owing to the occurrence of hydrophilic surface functional groups on the RSN

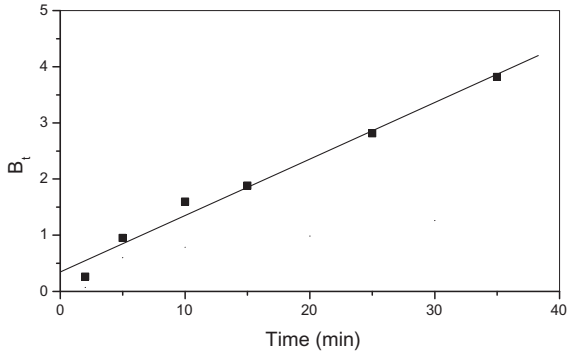

Fig. 6. Boyd plot of the kinetics for thorium sorption.

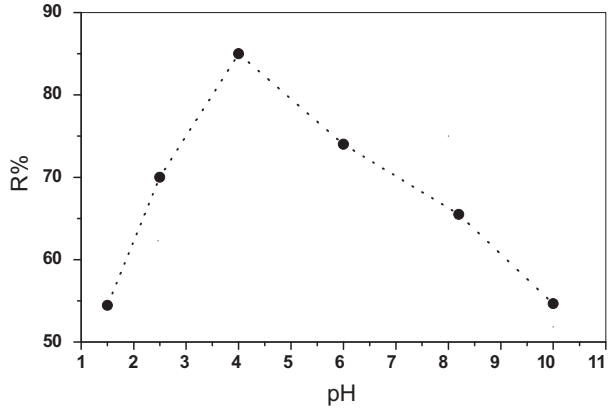

Fig. 8. Fractional thorium adsorption as function of pH.

carbon surface that can increase active sites' availability toward thorium ions. Fig. 9 gives thorium hydrolyzed species distribution curves. At pH 4, about 30% of Th^{4+} is free, 60% transformed to $Th(OH)_3^+$, and 10% transformed to $Th(OH)_2^{2+}$. The maximum uptake of thorium at pH 4.0 can be due to the development of monovalent $Th(OH)_3^+$ species, which is predominant at this pH.

Competition of thorium ions with H^+ ion for adsorption sites can be one of the main reasons for the reduction of its sorption at low pH. At low pH, adsorbent surface enclosed by hydronium ions that reduce interaction between thorium ions and binding sites on carbon surface by greater repulsive forces. In contrast, uptake decrease at high pH (pH > 4) is owing to the formation of $Th(CO_3)_5^{6-}$ and/or $Th(CO_3)_4^{4-}$ stable ions, which come from dissolution of atmospheric CO_2 and prevailing especially at alkaline medium [40,41].

3.7. Mechanism of radionuclide ion adsorption

Based on the earlier results, including RSN carbon characterization, and the information of thorium solution chemistry and its forms of adsorbed species, we can suggest a preliminary sorption mechanism. Treatment of the activated rice straw with HNO_3 increased acidic surface oxygen content and point of zero charge decreases. RSN carbon surface functional groups (such as –COOH, $–COO^-$, $–OH_2^+$, $–O^-$, –OH, etc.) take part in thorium adsorption. On one hand, presence of these acidic groups results in localization of basal planes π-electrons and increase its interaction with thorium ion species [43]. On the other hand, dissociation of these acidic functional groups on carbon surface can behave as a cation-exchanger in solution by which is essentially dependent upon their pka value. Acidic functional groups are not deprotonated at low pH that decrease thorium adsorption. On the contrary, at pH 4, dissociation of acidic groups, specially carboxylic groups (–COOH) is high and leads to an ion exchange adsorption on carbon surface [43].

The point of zero charge (pHpzc) of RSN carbon is 3 (Table 1). At pH < 3, the surface is positive and electrostatic repulsion leads to decreasing adsorption efficiency of Th(IV). At higher pH (>3), RSN carbon's surface becomes negative and electrostatic attraction increases, which enhances Th(IV) adsorption. Th(IV)'s complex characteristics that dominate at a particular solution pH could also play a significant role in the adsorption capacity of RSN carbon for thorium [34]. As we stated earlier, that formation of monovalent $Th(OH)_3^+$ species is predominant at pH 4, and it is responsible for increasing adsorption. Mainly, in comparison with divalent ions $Th(OH)_2^{2+}$ and tetravalent Th ions, the monovalent ions $Th(OH)_3^+$ have high ion-exchange capacity with protons on adsorbent since they can replace only one proton on distinct binding sites on the surface of adsorbent. Given the above characterization, a schematic diagram of the adsorption of Th(IV) to oxidized carbon can be drawn (Fig. 10). In this system, at low pH, hydrogen concentration is high that leads to protonation of ion-exchange sites and it is less available for ion exchange. At pH range 2.0–5.0, ion exchange is the main mechanism for thorium adsorption due to deprotonation of carboxylic groups. This was well supported by the result of decreasing pH after adsorption.

It is important to note that part of the thorium may enter slowly into the inner-channel of RSN

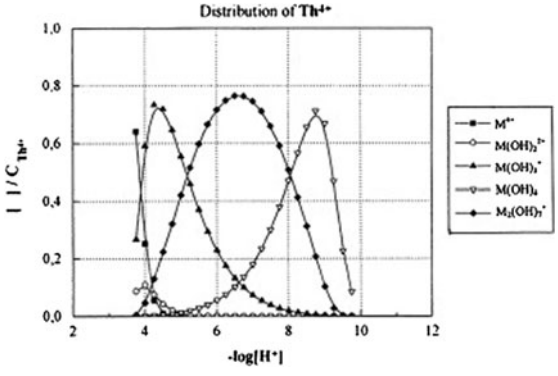

Fig. 9. Effect of pH on thorium species (10–4 mol/l) [42].

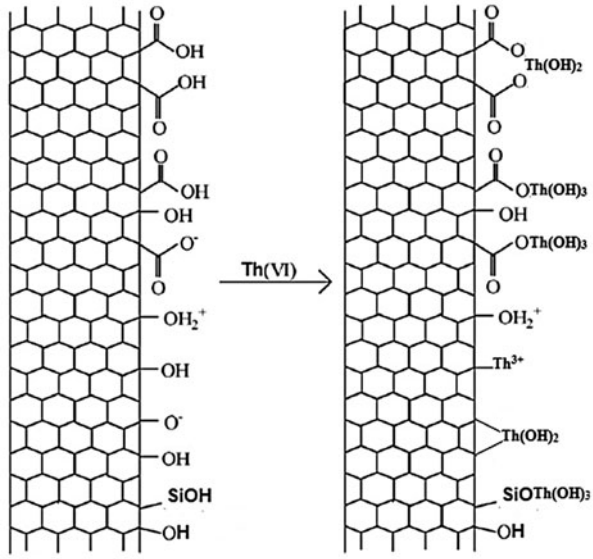

Fig. 10. A schematic diagram of main mechanism for thorium adsorption onto surface of activated carbon.

carbon at long contact adsorption time [44,45] due to the radius of Th(IV) ions being so small. These results are in line with that for chromium adsorption on oxidized carbon nanotubes [46].

3.8. Desorption of thorium

Adsorbent regeneration is a significant aspect in the treatment of wastewater. To investigate Th(IV) elution from the RSN carbon, desorption experiments were conducted using several desorping agents of 0.1 M of salt solution ($NaHCO_3$, Na_2CO_3), mineral acids (H_2SO_4, HNO_3, and HCl), and organic acids (acetic, oxalic). The results show that the desorption capacity (R_{des}%) of distilled water, $NaHCO_3$, HCl, HNO_3, H_2SO_4, acetic acid, and oxalic acid was 0.7, 28.2, 14.9, 17.2, 45.8, 0.6, and 15.4, respectively. According to these results, the lowest elution is done by distilled water and safe disposal of spent activated carbon. Further, these findings are in line with strong non-electrostatic interactions between carbon used and thorium ions. H_2SO_4 was found to be the most efficient desorbent eluent for thorium from RSN carbon. These chemicals could change adsorbed species chemical form and/or break the bond between them. Thus, thorium ion release from the RSN carbon surface.

Influence of different H_2SO_4 concentrations (up to 10 M) on thorium desorption efficiency from RSN carbon were also studied. Maximum desorption was achieved with 5 M H_2SO_4, which could be due to ion exchange mechanism. The lower thorium adsorption capacity at lower pH indicates that its desorption can be done in acidic solution.

Table 3
Thorium adsorption by different adsorbents

Adsorbent	q (mg/g)	Refs.
RSN	46.2	This work
Activated carbon prepared from olive stone	21.28	[47]
Activated carbon	55.7	[2]
Natural zeolites	69.6	[2]
Synthetic zeolites	164.7	[2]
Oxidized multi-wall carbon nanotubes	16.3	[48]
PAN/zeolite	9.28	[49]
Na-HEU-zeolite	30.2	[50]
AXAD-16 polymer	162.4	[51]
Amberlite XAD	26.2	[52]
Merrifield polymer–TTA	25.5	[53]
Silica SBA-15/ salicylaldimine	18.5	[54]
Amberlite XAD-4	69.6	[55]
Ignited Sarcotragus muscarum	5.1×10^{-4}	[56]

3.9. Comparison with some other adsorbents

Th(IV) adsorption by RSN carbon is compared with other adsorbents discussed in the literature (Table 3). Essentially, RSN carbon shows very good sorption performance for thorium in comparison with other adsorbents reported in the literature.

RSN carbon uptake capacity for thorium exceeded some of commercial ion exchange resin and activated carbon and comparable with others. Some ion exchangers show high thorium adsorption capacities. However, RSN carbon should be considered as preferred adsorbents due to reusability and low costs.

4. Conclusions

This investigation shows the efficiency of rice straw activated carbon oxidized with HNO_3 as a good and low-cost thorium adsorbent from aqueous solutions in a short time (120 min). Thorium adsorption onto RSN carbon reach its maximum at solution pH 4.0 and thorium concentration of 20 mg/l. Kinetics of adsorption followed pseudo-second-order proposing chemisorption and ion exchange nature of the process. Intra-particle is not an operative mechanism, and the Boyd kinetic expressions proposed particle diffusion to be the rate-limiting step. RSN carbon had comparable adsorption capacity for thorium as compared to other adsorbents. Thorium(IV) adsorbed can be professionally desorbed by 5 M H_2SO_4. In light of the current finding, HNO_3 oxidized activated carbon exhibits promising application in the field of nuclear science and technology for pre-concentration and solidification of thorium from large-volume solution treatments.

Acknowledgments

This project was supported by King Saud University, Deanship of Scientific Research, College of Science Research Center.

References

[1] B. Wierczinski, S. Helfer, M. Ochs, G. Skarnemark, Solubility measurements and sorption studies of thorium in cement pore water, J. Alloys Compd. 271–273 (1998) 272–276.
[2] M. Metaxas, V. Kasselouri-Rigopoulou, P. Galiatsatou, C. Konstantopoulou, D. Oikonomou, Thorium removal by different adsorbents, J. Hazard. Mater. 97 (2003) 71–82.
[3] D. Alipour, A.R. Keshtkar, M.A. Moosavian, Adsorption of thorium(IV) from simulated radioactive solutions using a novel electrospun PVA/TiO_2/ZnO nanofiber adsorbent functionalized with mercapto

groups: Study in single and multi-component systems, Appl. Surf. Sci. 366 (2016) 19–29.
[4] Y. Yamazaki, Y. Tachibana, T. Kaneshiki, M. Nomura, T. Suzuki, Adsorption behavior of uranium ion using novel phenol-type resins in contaminated water containing seawater, Prog. Nucl. Energy 82 (2015) 74–79.
[5] M.W. Munthali, E. Johan, H. Aono, N. Matsue, Cs^+ and Sr^{2+} adsorption selectivity of zeolites in relation to radioactive decontamination, J. Asian Ceram. Soc. 3 (2015) 245–250.
[6] L. Zhang, J. Wei, X. Zhao, F. Li, F. Jiang, Adsorption characteristics of strontium on synthesized antimony silicate, Chem. Eng. J. 277 (2015) 378–387.
[7] W. Liu, X. Zhao, T. Wang, D. Zhao, J. Ni, Adsorption of U(VI) by multilayer titanate nanotubes: Effects of inorganic cations, carbonate and natural organic matter, Chem. Eng. J. 286 (2016) 427–435.
[8] L. Zhang, J. Wei, X. Zhao, F. Li, F. Jiang, M. Zhang, X. Cheng, Competitive adsorption of strontium and cobalt onto tin antimonate, Chem. Eng. J. 285 (2016) 679–689.
[9] S.M. Yakout, Effect of porosity and surface chemistry on the adsorption-desorption of uranium(VI) from aqueous solution and groundwater, J. Radioanal. Nucl. Chem. 308 (2016) 555–565.
[10] S. Biniak, G. Szymański, J. Siedlewski, A. Świątkowski, The characterization of activated carbons with oxygen and nitrogen surface groups, Carbon 35 (1997) 1799–1810.
[11] A.A.M. Daifullah, S.M. Yakout, S.A. Elreefy, Adsorption of fluoride in aqueous solutions using $KMnO_4$-modified activated carbon derived from steam pyrolysis of rice straw, J. Hazard. Mater. 147 (2007) 633–643.
[12] A.W. Heinen, J.A. Peters, H. Bekkum, Competitive adsorption of water and toluene on modified activated carbon supports, Appl. Catal. A: General 194–195 (2000) (2000) 193–202.
[13] J.W. Shim, S.J. Park, S.K. Ryu, Effect of modification with HNO_3 and NaOH on metal adsorption by pitch-based activated carbon fibers, Carbon 39 (2001) 1635–1642.
[14] C.A. Leon y Leon, J.M. Solar, V. Calemma, L.R. Radovic, Evidence for the protonation of basal plane sites on carbon, Carbon 30 (1992) 797–811.
[15] T.J. Bandosz, J. Jagiello, J.A. Schwarz, Comparison of methods to assess surface acidic groups on activated carbon, Am. Chem. Soc. 64 (1992) 891–895.
[16] S.S. Metwally, B. El-Gammal, H.F. Aly, S.A. Abo-El-Enein, Removal and separation of some radionuclides by poly-acrylamide based Ce(IV) phosphate from radioactive waste solutions, Sep. Sci. Technol. 46(11) (2011) 1808–1821.
[17] W. Song, M. Guo, Quality variations of poultry litter biochar generated at different pyrolysis temperatures, J. Anal. Appl. Pyrolysis 94 (2012) 138–145.
[18] H.P. Boehm, Some aspects of the surface chemistry of carbon blacks and other carbons, Carbon 32 (1994) 759–769.
[19] E. Guibal, C. Roulph, P. Le Cloirec, Uranium biosorption by a filamentous fungus Mucor miehei pH effect on mechanisms and performances of uptake, Water Res. 26 (1992) 1139–1145.
[20] H.H. Tran, F.A. Roddick, J.A. O'Donnell, Comparison of chromatography and desiccant silica gels for the adsorption of metal ions—I. Adsorption and kinetics, Water Res. 33 (1999) 2992–3000.
[21] B. Volesky, Biosorption of Heavy Metals, CRC Press, Boca Raton, FL, 1990.
[22] Y.B. Tang, F.Y. Chen, H.L. Zhang, Adsorption of Pb^{2+}, Cu^{2+} and Zn^{2+} ions on to waste fluidized catalytic cracking (FCC) catalyst, Adsorp. Sci. Technol. 16 (1998) 595–606.
[23] Y.S. Ho, G. McKay, The kinetics of sorption of divalent metal ions onto sphagnum moss peat, Water Res. 34 (2000) 735–742.
[24] M. Chairat, S. Rattanaphani, J.B. Bremner, V. Rattanaphani, An adsorption and kinetic study of lac dyeing on silk, Dyes Pigm. 64 (2005) 231–241.
[25] K. Anoop Krishnan, T.S. Anirudhan, Removal of mercury(II) from aqueous solutions and chlor-alkali industry effluent by steam activated and sulphurised activated carbons prepared from bagasse pith: Kinetics and equilibrium studies, J. Hazard. Mater. 92 (2002) 161–183.
[26] M.-S. Chiou, H.-Y. Li, Equilibrium and kinetic modeling of adsorption of reactive dye on cross-linked chitosan beads, J. Hazard. Mater. 93 (2002) 233–248.
[27] D. Mohan, K.P. Singh, Single- and multi-component adsorption of cadmium and zinc using activated carbon derived from bagasse—An agricultural waste, Water Res. 36 (2002) 2304–2318.
[28] A.K. Chaturvedi, K.C. Pathak, V.N. Singh, Fluoride removal from water by adsorption on china clay, Appl. Clay Sci. 3 (1988) 337–346.
[29] W.J. Weber, J.C. Morris, J. Sanit, Kinetics of sorption of carbon from solution, Journal of the Sanitary Engineering Division, Am. Soc. Civ. Eng. 89 (1963) 31–60.
[30] F.-C. Wu, R.-L. Tseng, R.-S. Juang, Comparisons of porous and adsorption properties of carbons activated by steam and KOH, J. Colloid Interface Sci. 283 (2005) 49–56.
[31] Y.-S. Ho, Removal of copper ions from aqueous solution by tree fern, Water Res. 37 (2003) 2323–2330.
[32] S. Venkata Mohan, N. Chandrasekhar Rao, J. Karthikeyan, Adsorptive removal of direct azo dye from aqueous phase onto coal based sorbents: A kinetic and mechanistic study, J. Hazard. Mater. 90 (2002) 189–204.
[33] G.E. Boyd, A.W. Adamson, L.S. Myers Jr., The exchange adsorption of ions from aqueous solutions by organic zeolites. II. Kinetics1, J. Am. Chem. Soc. 69 (1947) 2836–2848.
[34] D. Reichenburg, Properties of ion-exchange resins in relation to their structure, J. Am. Chem. Soc. 75 (1972) 589–597.
[35] M.S. El-Shahawi, A.M. Othman, H.M. Nassef, M.A. Abdel-Fadeel, An investigation into the retention profile and kinetics of sorption of the ternary complex ion associate of uranyl ions with crown ether and picric acid by the polyurethane foams, Anal. Chim. Acta 536 (2005) 227–235.
[36] K.V. Kumar, V. Ramamurthi, S. Sivanesan, Modeling the mechanism involved during the sorption of methylene blue onto fly ash, J. Colloid Interface Sci. 284 (2005) 14–21.
[37] A. Seco, P. Marzal, C. Gabaldón, Study of the adsorption of Cd and Zn onto an activated carbon: Influence of pH, cation concentration, and adsorbent concentration, Sep. Sci. Technol. 34 (1999) 1577–1593.

[38] S. Akyil, M.A.A. Aslani, M. Eral, Sorption characteristics of uranium onto composite ion exchangers, J. Radioanal. Nucl. Chem. 256 (2003) 45–51.
[39] M.A. Aslani, S. Akyil, M. Eral, Thorium(IV) sorption on ignited *Sarcotragus muscarum*, its kinetic and thermodynamic parameters, J. Radioanal. Nucl. Chem. 250 (2001) 153–157.
[40] C. Kütahyalı, M. Eral, Selective adsorption of uranium from aqueous solutions using activated carbon prepared from charcoal by chemical activation, Sep. Purif. Technol. 40 (2004) 109–114.
[41] E. Piron, A. Domard, Interaction between chitosan and uranyl ions, Int. J. Biol. Macromol. 21 (1997) 327–335.
[42] E. Bentouhami, G.M. Bouet, J. Meullemeestre, F. Vierling, M.A. Khan, Physicochemical study of the hydrolysis of Rare-Earth elements (III) and thorium (IV), C.R. Chim. 7 (2004) 537–545.
[43] P. Galiatsatou, M. Metaxas, V. Kasselouri-Rigopoulou, Adsorption of zinc by activated carbons prepared from solvent extracted olive pulp, J. Hazard. Mater. 91 (2002) 187–203.
[44] X. Wang, C. Chen, W. Hu, A. Ding, D. Xu, X. Zhou, Sorption of ^{243}Am(III) to multiwall carbon nanotubes, Environ. Sci. Technol. 39 (2005) 2856–2860.
[45] G. Hummer, J.C. Rasaiah, J.P. Noworyta, Water conduction through the hydrophobic channel of a carbon nanotube, Nature 414 (2001) 188–190.
[46] J. Hu, C. Chen, X. Zhu, X. Wang, Removal of chromium from aqueous solution by using oxidized multiwalled carbon nanotubes, J. Hazard. Mater. 162 (2009) 1542–1550.
[47] C. Kütahyalı, M. Eral, Sorption studies of uranium and thorium on activated carbon prepared from olive stones: Kinetic and thermodynamic aspects, J. Nucl. Mater. 396 (2010) 251–256.
[48] C. Chen, X. Li, D. Zhao, X. Tan, X. Wang, Adsorption kinetic, thermodynamic and desorption studies of Th (IV) on oxidized multi-wall carbon nanotubes, Colloids Surf. A: Physicochem. Eng. Aspects 302 (2007) 449–454.
[49] A.K. Kaygun, S. Akyil, Study of the behaviour of thorium adsorption on PAN/zeolite composite adsorbent, J. Hazard. Mater. 147 (2007) 357–362.
[50] P. Sharma, M. Sharma, R. Tomar, Na-HEU zeolite synthesis for the removal of Th(IV) and Eu(III) from aqueous waste by batch process, J. Taiwan Inst. Chem. Eng. 44 (2013) 480–488.
[51] M. Akhila Maheswari, M.S. Subramanian, Extraction chromatographic method for the separation of actinides and lanthanides using EDHBA grafted AXAD-16 polymer, Talanta 65 (2005) 735–742.
[52] S. Seyhan, M. Merdivan, N. Demirel, Use of o-phenylene dioxydiacetic acid impregnated in Amberlite XAD resin for separation and preconcentration of uranium(VI) and thorium(IV), J. Hazard. Mater. 152 (2008) 79–84.
[53] P.R. Vasudeva Rao, S.K. Patil, A spectrophotometric method for the determination of neptunium and plutonium in process solutions, J. Radioanal. Chem. 42 (1978) 399–410.
[54] L. Dolatyari, M.R. Yaftian, S. Rostamnia, Adsorption characteristics of Eu(III) and Th(IV) ions onto modified mesoporous silica SBA-15 materials, J. Taiwan Inst. Chem. Eng. 60 (2016) 174–184.
[55] N. Demirel, M. Merdivan, N. Pirinccioglu, C. Hamamci, Thorium(IV) and uranium(VI) sorption studies on octacarboxymethyl-C-methylcalix[4]resorcinarene impregnated on a polymeric support, Anal. Chim. Acta 485 (2003) 213–219.
[56] M. Eral, Thorium(IV) sorption on ignited Sarcotragus muscarum, its kinetic and thermodynamic parameters, J. Radioanal. Nucl. Chem. 250 (2001) 153–157.